2014 23rd International Lightning Detection Conference
18 - 19 March • Tucson, Arizona, USA
5th International Lightning Meteorology Conference
20 - 21 March • Tucson, Arizona, USA

Optical evidences of the inception mechanisms of natural bipolar cloud-to-ground lightning

Saraiva A. C. V., Campos L. Z. S., Zepka G. S., Alves J., Pinto Jr. O., Buzato T. S.
ELAT/CCST, Atmospheric Electricity Group
INPE, National Institute for Space Research
São José dos Campos, SP, Brazil
e-mail: acvsaraiva@gmail.com

Williams E. R.
Parsons Laboratory
Massachusetts Institute of Technology
Cambridge, MA, USA

Heckman S.
Earth Networks
Germantown, MD, USA

Bailey J. C.
Earth System Science Center
University of Alabama in Huntsville
Huntsville, AL, USA

Morales C. A.
IAG, Instituto de Astronomia, Geofísica e Ciências Atmosféricas
USP, Universidade de São Paulo
São Paulo, SP, Brazil

Blakeslee R. J.
NASA Marshall Space Flight Center
Huntsville, AL, USA

Abstract— **High-speed video records of two bipolar cloud-to-ground flashes were analyzed in detail. They were both initiated by single positive return strokes and were followed by more than one subsequent negative stroke. Due to the elevated cloud-base height of its parent thunderstorm, the initiation processes of each subsequent stroke could be registered optically below cloud base. In the first event (Case 1) it was possible to observe that all four subsequent negative strokes were initiated by recoil leaders that retraced one horizontal channel segment previously ionized by the positive leader that preceded the first stroke. Those recoil leaders connected to the original vertical channel segment and propagated towards ground, producing four subsequent strokes that had the same ground contact point of the original positive discharge. The second event (Case 2), on the other hand, presented fifteen subsequent strokes that were initiated by recoil leaders that did not reach the original channel of the positive stroke. They diverged vertically towards ground, making contact approximately 11 kilometers away from the original positive strike point. These are the first optical evidences that both single- and multiple-channel bipolar flashes occur as a consequence of recoil leader activity in the branches of the initial positive return stroke. For both events their total channel length increased progressively with time at a growth rate equivalent to a propagation speed of the order of 10^4 m/s, comparable to those reported for typical positive leaders.**

Keywords— Lightning; Bipolar Lightning; High-Speed Cameras; Lightning Location Systems; Inception Mechanism

Sponsored by FAPESP (Fundação de Apoio a Pesquisa do Estado de São Paulo) under grant numbers 08/56711-4, 2010/01742-2 and partially by 2009/15235-8.

I. INTRODUCTION

Bipolar lightning discharges are those that transfer both positive and negative electric charges to ground throughout their development. They are arguably one of the rarest types of lightning. In a review paper on this subject, Rakov [2003] discusses three basic categories of bipolar event. For upward and rocket-triggered lightning, he reports (i) events characterized by one or more polarity reversals during slowly varying current components [e.g., McEachron, 1939; Hubert et al., 1984; Waldteufel et al., 1980], (ii) events in which the initial-stage current and the following return strokes exhibit opposite polarities [e.g., Berger and Vogelsanger, 1966; Nakahori et al., 1982], and finally, the focus of the present paper, (iii) those events that present return strokes of both polarities [e.g., McEachron, 1939; Berger and Vogelsanger, 1965; Idone et al., 1987]. Rakov [2003] mentions that all documented discharges of the third type, at the time of publication, were of upward nature, with the exception of Idone et al. [1987]. They reported one case of triggered lightning initiated by the rocket-trailing wire technique that produced return strokes of both polarities. Four recent published reports [Fleenor et al., 2009; Jerauld et al., 2009; Nag and Rakov, 2012; Saba et al., 2013] document natural Cloud-to-Ground (CG) flashes that produce return strokes of both polarities. Most studies in the literature (including the present work) report the majority of natural downward bipolar flashes starting with a positive discharge.

The formation mechanism of natural downward bipolar flashes is discussed by Saba et al. [2013]. The authors suggest that the subsequent negative strokes are initiated by recoil leaders, according to the dart leader mechanism of the bidirectional leader concept [Kasemir, 1950, 1960; Mazur, 2002]. However, the lack of additional instrumentation and no conclusive optical evidence for this process left the discussion still open.

In the present work we report high-speed camera records and electromagnetic data of two unusual bipolar CG events in which the initiation of the subsequent negative strokes are visible below cloud base. The optical signatures of the processes that initiate the subsequent strokes are similar to the recoil leader phenomenology present in the literature [Mazur, 2002; Saba et al., 2008; Mazur and Ruhnke, 2011; Campos et al., 2014].

II. INSTRUMENTATION

During the summer of 2011/2012 the first lightning observation campaign of the RAMMER network (acronym in Portuguese for "Automatized multi-camera network to observe and study lighting" [Saraiva et al., 2011]) was conducted in São José dos Campos, SP, Brazil. Over the same period, the CHUVA project (Cloud processes of the main precipitation systems in Brazil: A contribution to cloud resolving modeling and to the Global Precipitation Measurement [Machado et al., 2012]) installed several lightning detection systems covering the same region. The joint experiment led to a unique dataset of lightning measurements. The cases presented here were observed by one RAMMER sensor and BrasilDAT network [Naccarato et al., 2012], with additional lightning location data from the CHUVA Vale do Paraíba experiment (LINET, GLD360 and TLS200). Information provided by the LMA (Lightning Mapping Array) network established for the CHUVA campaign was also used. The next sections will present a brief description of the instruments used in this analysis.

A. RAMMER Network

The RAMMER network was developed at the Brazilian National Institute for Space Research, sponsored by FASPESP (Fundação de Amparo à Pesquisa do Estado de São Paulo), beginning in late 2010. Each sensor consists of a high-speed camera, computer, GPS antenna, and some control circuitry. All equipment is stored in a weatherproof box, allowing it to be installed virtually anywhere.

The camera is a Phantom V9.1, manufactured by Vision Research, and was configured for video records of two-second duration at 2500 frames per second (fps) with a maximum exposure time of 390 µs. The spatial resolution is 1200 x 500 pixels, with 8-bit pixel depth (256 gray levels). This set up generates a video file of about 3 GB, and requires about 2 minutes to be transferred from the camera to the computer. During these 2 minutes no other flash can be recorded.

Two sensors were installed in São José dos Campos during that summer season and the operation began on November 30th, 2011, and ended on March 30th, 2012. Figure 1 shows the locations of the sensors during March 13th, 2012, and the markers show the locations of the case study flashes. As the events occurred behind the RAMMER 1 sensor, only RAMMER 2 was able to record them.

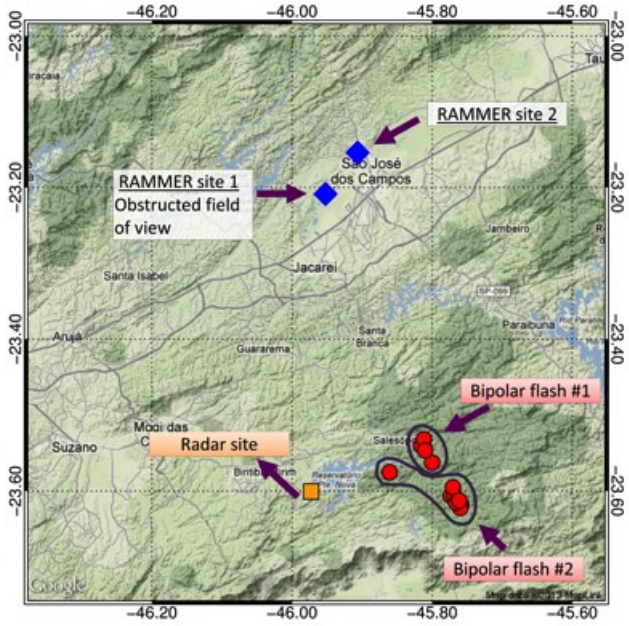

Fig. 1. Relative locations of the camera observation site, radar and the LLS solutions for the detected strokes of both analyzed events. The blue diamonds are the location of the RAMMER sites installed during the summer of 2011/2012. The red circles are the estimated locations of each stroke of the bipolar CG flashes and the yellow square is the location of the radar used in this work.

B. Lightning detection networks

For the return strokes recorded by the high-speed cameras, some had their locations and peak currents estimated by the Lightning Location Systems (LLS) in operation during that summer. Brazil has two fixed low frequency (LF) based networks: RINDAT (comprised of Vaisala sensors) and BrasilDAT (EarthNetworks sensors). The LF-based networks provide estimates of location, time of occurrence and return stroke peak current. Waveforms of the sensor closest to the events were retrieved from EarthNetworks database, enabling us to recalculate peak currents more precisely and even estimate peak currents of strokes not detected by any other LLS that were operational during the CHUVA experiment. Moreover, during the CHUVA GLM Vale do Paraiba campaign, LINET [Betz et al., 2004] and a TLS200 network (from Vaisala), were also installed. The GLD 360 VLF network [Demetriades et al., 2010] also provides peak current estimates.

C. Lightning Mapping Array system

A temporary network of LMA receivers had been installed around the São Paulo metropolitan area during the 2011/2012 summer season. The network, named SPLMA, consisted of 12 sensors developed by the New Mexico Institute of Mining and Technology [Rison et al., 1999]. They were designed to detect lightning electromagnetic sources in the VHF range and locate them three-dimensionally, making it possible to map the channel development both inside and outside the cloud. Both

bipolar CG flashes analyzed in the present work occurred outside the network area, at distances ranging from 87 to 97 km from the LMA coordinate center. The VHF source locations were used as complementary data to the high-speed video observations of the bipolar CG events detailed in the present paper.

III. Analyses and Results

During March 13th several single and multicellular thunderstorms formed in the observation region (over São Paulo metropolitan area and Vale do Paraíba). At 16:50 UT, a complex, multicellular thunderstorm began to develop northeast of the radar site and 50 km south of the camera site, in the form of an east-west-oriented squall line. The RAMMER network registered a total of 44 CG flashes, the highest number for a single day during the campaign. However, the most impressive behavior occurred between 20:10 UT and 20:33 UT, when the camera registered two bipolar CG flashes in a 3-minute interval, followed by 4 positive CG flashes. Such behavior has never observed in that region during more than 10 years of high-speed camera observations. The camera observed no negative flashes within this period, aside from the negative subsequent strokes in the bipolar CG flashes. All six flashes recorded in this period presented intense recoil leader activity visible below cloud base and, as discussed in the following sections, with some of them also responsible for the formation of subsequent negative strokes in the bipolar CG cases. Figure 2 is a radar CAPPI (Constant Altitude Plan Position Indicator) image at 20:14 UT, less than one minute after the second bipolar CG flash that was recorded, showing the complex structure of the thunderstorm at that time.

A photogrammetry of the images, combined with the positions of the discharges estimated by the LLS, allowed the calculation of several parameters, like the cloud base height (above ground level) and channel length. The estimated cloud base height was 3.2 km, which is close to the value given by the nearby sounding (2.7 km), and also consistent with elevated cloud base heights in the case of mesoscale trailing stratiform regions [Zipser, 1977]. The channel length was calculated assuming that the horizontal propagation of the channels is perpendicular to the camera detector. Only the visible portion of the channel was considered in the calculations. BrasilDAT network data was used for location purposes for this analysis since its sensors are more uniformly distributed around the lightning events of interest than the other smaller networks that were operational during CHUVA. The average location error evaluated based on these events was around 1.5 km.

The following sections will discuss the formation and characteristics of the two bipolar CG flashes, which will be referred to as Case 1 and Case 2.

A. Case 1 description

Case 1 occurred at 20:10:50 (UT) and was the first bipolar CG flash recorded on 03/13/2012. An overview of selected video camera frames from Case 1 is presented in Figure 3, showing the visible channel of each return stroke. In order to maximize the information provided by the BrasilDAT sensors, the waveforms corresponding to both cases were retrieved from the closest sensor to the lightning flashes for a thorough manual evaluation. Most of the strokes that were not reported by any LLS were identified on the waveforms and had their E-field peak values used to estimate their corresponding peak currents. All recalculated peak currents for Case 1 are presented in Table 1. Figure 4 show the waveforms for all five strokes that compose Case 1; time t=0 represent the moment of the positive return stroke (20:10:50.943396 UT) and the subsequent time steps are presented in milliseconds. The waveforms also provide confirmation of the polarity change on the subsequent return strokes.

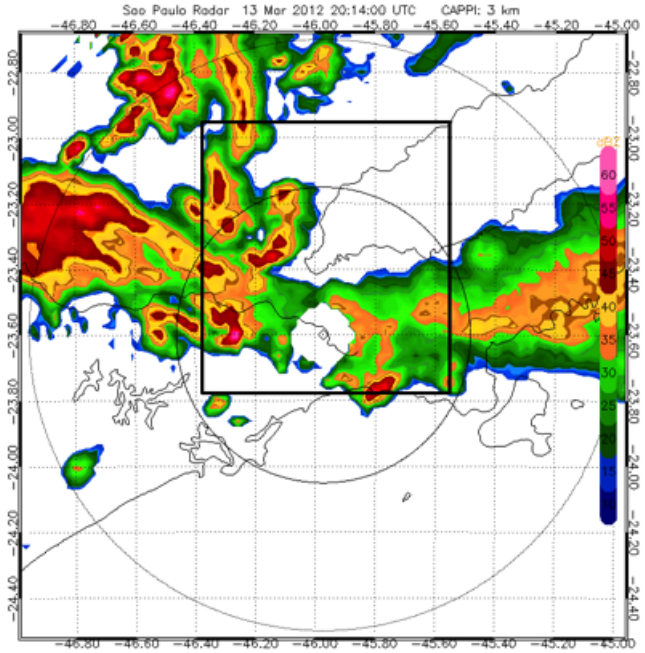

Fig. 2. Constant Altitude Plan Position Indicator (CAPPI) at 3 km height less than one minute after Case 2 was recorded, at 20:14:00 UTC. The black square indicates the same area presented in Figure 1.

The initial stroke of the flash had positive polarity, which was set up by a positive leader whose development was accompanied by a large number of recoil leaders visible below cloud base. A continuing current of approximately 33 milliseconds followed it. The estimated ground strike point was 44 km from the camera, as calculated by using the LLS solutions and the GPS location of the observation site.

At time t = 168.4 ms the first negative return stroke was observed, initiated by one of the recoil leaders that could be observed approximately 2 ms prior to it. It was initiated in a horizontal channel branch that had been progressively developed by the propagating positive leader, as indicated by a large number of sequential recoil leaders that occurred at different moments after time t = 4 ms (when recoil activity first became visible below cloud base). Prior the initiation of the first negative return stroke, almost twenty intense individual recoil leaders could be identified to occur in channel segments that later on became part of the stroke. Figure 5 shows the luminosity (pixel values) *versus* time plot of a rectangular box of the video frames, set over that region which includes a channel segment that is common to all negative return strokes and the aforementioned sequence of recoil leaders. All three

subsequent return strokes used the same channel as the first negative stroke and the progression of the horizontal leader was clearly observed. They were also initiated by a recoil/dart leader processes.

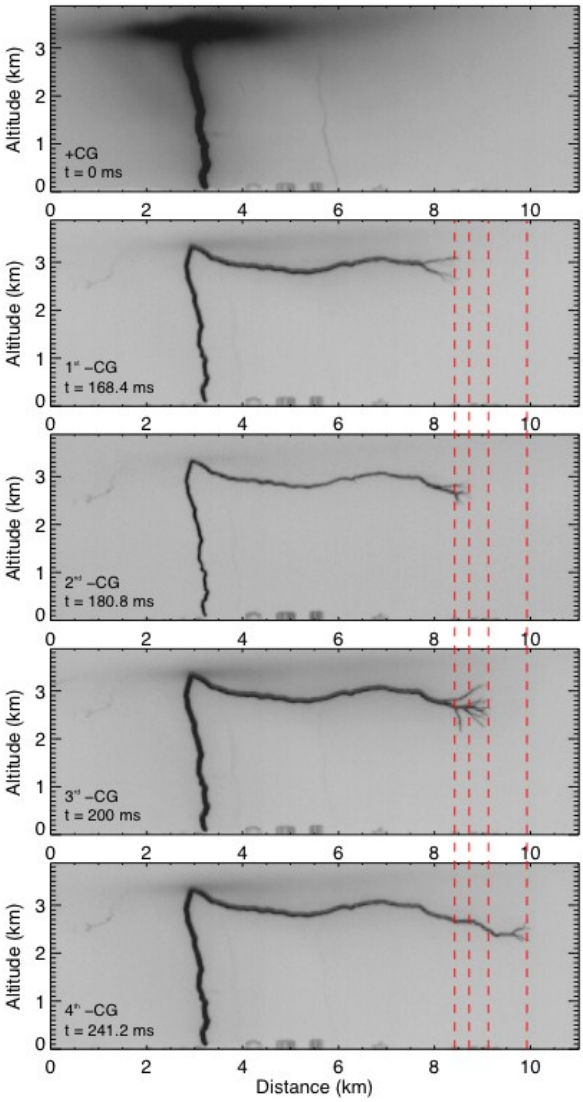

Fig. 3. Selection of frame negatives for the return strokes comprising Case 1. The red dashed lines show the growth of channel length with time and stroke order.

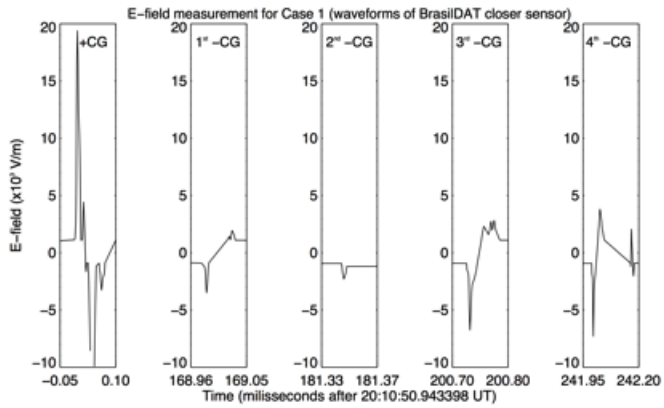

Fig. 4. Electric field waveforms extracted from the BrasilDAT sensor that was closest to Case 1 ground strike point. Each graph shows a few microseconds of data for each return stroke.

The general characteristics of each recoil/dart leader-return stroke sequence are summarized in Table 1. The photogrammetric analysis also allowed rough estimates of the average speeds of the recoil/dart leader processes of all the negative strokes of Case 1. They ranged from 4.5 x 10^6 to 1.3 x 10^7 m/s, in agreement with previous reports of both dart [Schonland et al., 1935; Orville and Idone, 1982; Jordan et al., 1992; Campos et al., 2014] and recoil leader [Shao et al., 1995; Saba et al., 2008] speeds from digital high-speed cameras.

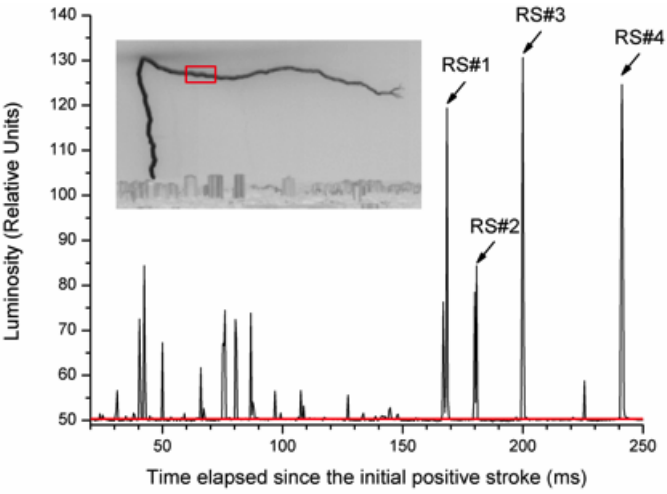

Fig. 5. Luminosity versus time plot of the pixels located inside the red rectangle, showing the occurrence and relative intensity of the recoil leaders and negative subsequent strokes of Case 1 (indicated as RS#1 through RS#4).

TABLE I. SUMMARY OF CHARACTERISTICS OF EACH OF THE FOUR RETURN STROKES OBSERVED IN CASE 1. IP CORRESPONDS TO THE PEAK CURRENTS, D IS THE DISTANCE BETWEEN THE STROKES AND THE CAMERA, LTOTAL IS THE TOTAL VISIBLE CHANNEL LENGTH AND RL/DL SPEED IS THE ESTIMATED EXTENSION SPEED OF THE RECOIL/DART LEADER SEQUENCE THAT INITIATED EACH STROKE. N/A STANDS FOR NO DATA AVAILABLE.

Order	**Time of occurrence (UT)**	**I_p (kA)**			**D (km)**	**L_{total} (m)**	**RL/DL speed (x10^6 m/s)**
		BrasilDAT	***GLD360***	***TLS200***			
Positive	20:10:50.944s (t = 0)	+24.2	+27.4	+25.0	43.9	3480	-
1	51.113s (t = 168.4 ms)	–4.38	-	-	46.7	8890	4.45
2	51.125s (t = 180.8 ms)	–2.87	-	-	-	9100	7.58
3	51.144s (t = 200.0 ms)	–8.43	-	–6.70	43.1	9510	7.92
4	51.186s (t = 241.2 ms)	–9.11	-	–7.60	44.8	10450	1.31

Through a simple visual inspection of each return stroke frame (Figure 3) it was noticeable that the total channel length increased with stroke order as the recoil/dart leader processes had inception points progressively more distant from the vertical segment created by the initial positive stroke. This evolution is presented graphically in Figure 6, which shows the total visible channel length (L_{total} in Table I) *versus* time elapsed since the initial positive return stroke. Despite the small number of points available for Case 1, it is noticeable that there is a linear correlation between the two parameters. By fitting the data linearly, the obtained slope is 22 m/ms, which can be interpreted as the recoil/dart leader inception points are moving away from the vertical channel segment with a speed of 2.2 x 10^4 m/s, resulting in progressively longer channels as each subsequent stroke occur. Given the statistical data presented by Saba et al. [2008] and Campos et al. [2014], this speed is in good agreement with the lower end of the distribution of natural positive leader speeds. The speed estimate is remarkably similar to the value obtained by Waldteufel et al. [1980] for the upward propagation of the stroke extremities of a triggered lightning flash that had its entire development visible below cloud base (3 x 10^4 m/s). Although the polarity of the leader could not be determined conclusively, the magnitude of its speed suggests positive polarity.

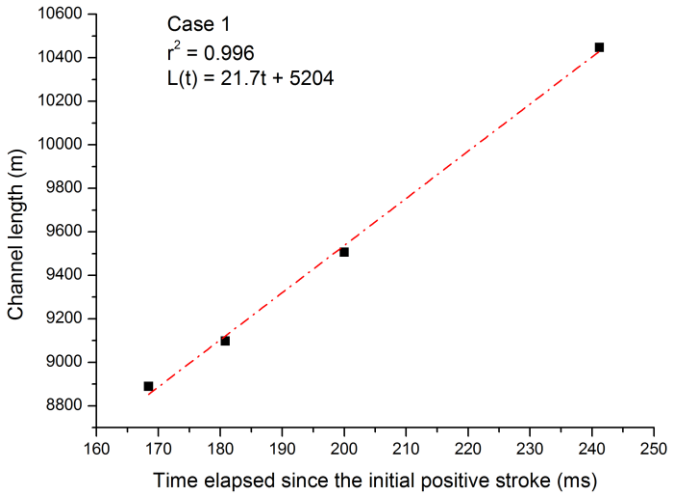

Fig. 6. Total visible channel length (as estimated from the photogrammetric analysis) *versus* time elapsed since the initial positive return stroke for Case 1. Each square corresponds to one of the four negative strokes.

Figure 7 shows plots of VHF sources mapped by SPLMA for Case 1. The '+' symbols denote the location and/or time of occurrence of each return stroke, as provided by the both high-speed camera recordings and the solutions from the LF networks. The first noticeable feature is the good position and timing match between the LF solutions and the distributions of VHF sources. The plot of source rate versus time shows that the majority of available points correspond to the in-cloud development of strongly VHF-emissive negative leaders as part of the bipolar formation of the initial positive return stroke. Even after the cessation of its continuing current (which lasted approximately 33 milliseconds) and throughout the occurrence of the following four negative strokes, a large number of VHF sources are located above 5 km altitude (present in the number of sources versus height). The plots also show a considerable decrease in the number of sources approximately 10 milliseconds prior to the first subsequent negative stroke at t = 168.4 ms. This suggests that there is no apparent connection between the negative strokes and the in-cloud development, or at least that their occurrence had no effect in intensifying it. The sources detected temporally close to the fourth subsequent stroke do not seem to be connected to it because of their spatial separation: there are no detections below 5 km and the latitude versus longitude diagram in Figure 7 indicates that they were produced further west from the ground contact points. This rough independence between strokes to ground and in-cloud development was also reached by Krehbiel et al. [1979, p. 21] and Krehbiel [1981, p. 224] for both intracloud and cloud-to-ground flashes based on multiple-station slow electric field data.

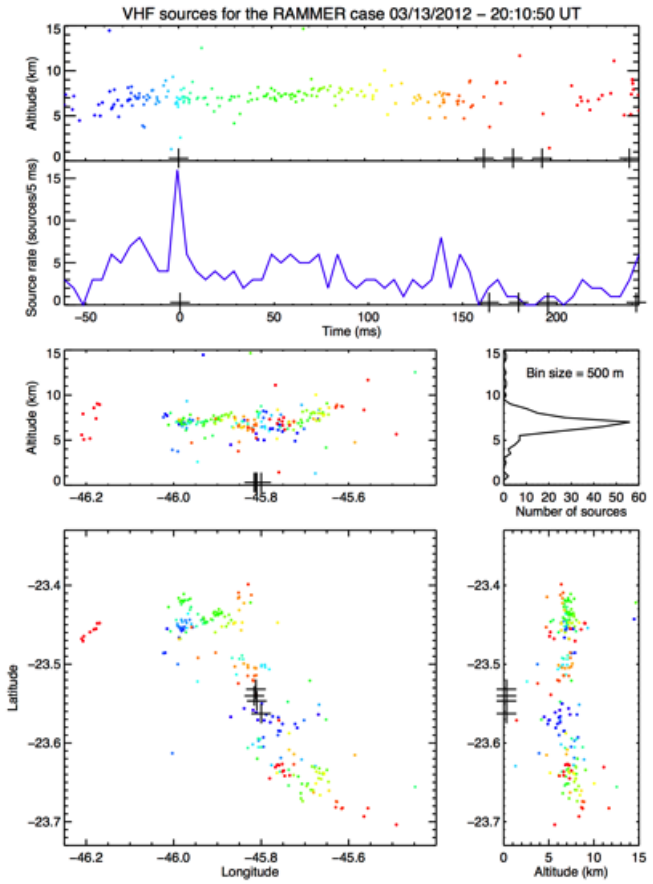

Fig. 7. Plot of VHF sources produced by Case 1 and mapped by the SPLMA. Time progression is color coded according to the two topmost panels (altitude and source rate versus time plots). Each one of the other panels corresponds to spatial projections of the radiation source locations and the '+' symbols indicate the location and/or time of occurrence of each return stroke (provided by the high-speed camera and LF network solution data).

B. Case 2 description

Case 2 began at 20:13:46 (UT) as the second bipolar CG flash observed by the RAMMER station camera. It occurred approximately 3 minutes later than Case 1. Similar to Case 1, Case 2 was initially of positive polarity, with estimated ground contact (based on the camera records) at 20:13:45.905596 (UT)

and was followed by fifteen subsequent negative strokes. Figure 8 presents a selection of video frames showing some of the return strokes that comprise Case 2. Similar to Case 1, the waveforms related to this flash were retrieved from a BrasilDAT sensor and waveforms for a selection of return strokes are displayed in Figure 9, also confirming the change of polarity between return strokes. Contrary to Case 1, the video record of the positive leader that produced the conductive path to ground did not show visible recoil activity below cloud base, possibly because of the larger distance from the camera. The four LF networks provided solutions for the positive stroke, whose ground contact point was estimated to be approximately 47 km away from the camera. There was a persistence of the channel luminosity that lasted approximately 95 milliseconds, very close to the median value for the duration of continuing currents of positive strokes (97 ms, according to Saba et al. [2010]).

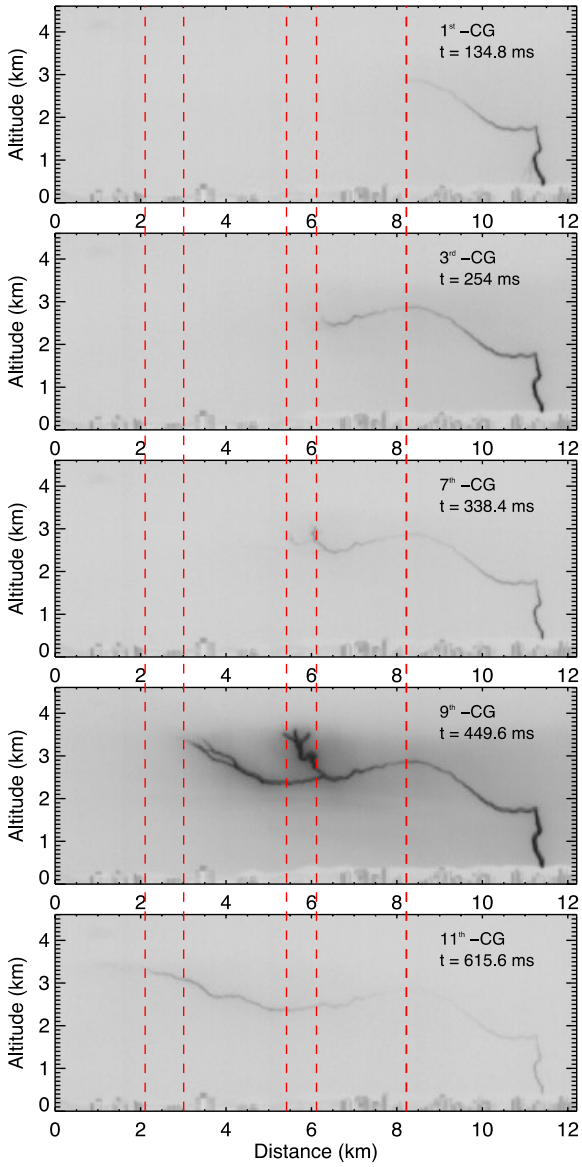

Fig. 8. Selected negative frames of some of the negative strokes for Case 2. The red dashed lines show the growth of channel length with time and stroke order.

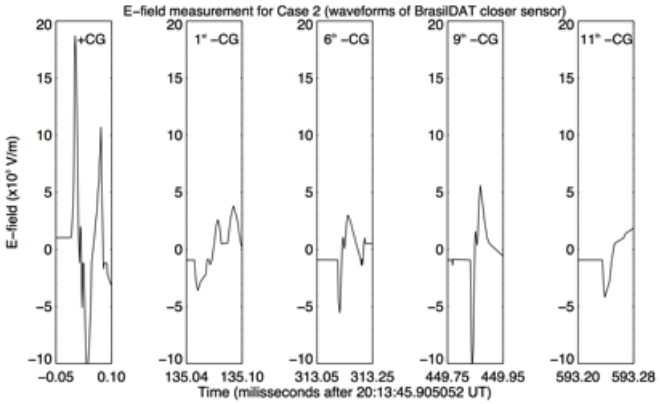

Fig. 9. Same as in Figure 4, but only some of the return stroke waveforms for Case 2 are shown. The positive stroke is the first graph, followed by the first negative CG, then the 6th, 9th and 11th –-CGs.

The instant the initial positive return stroke occurred will be taken as time t = 0. At t = 134.8 ms (roughly 40 milliseconds after the cessation of the continuing current) another return stroke occurred. During the time interval between the initial positive stroke and its first subsequent stroke the camera indicated some recoil activity both within the cloud (mostly diffuse in the video camera imagery) and below its base (with discernible channels). The solutions provided by the LF networks indicate that the ground contact point of the first subsequent stroke was approximately 53 kilometers from the camera and separated from the initial positive stroke by about 11 km. Approximately 6 milliseconds before the first subsequent return stroke some recoil activity was visible, but the exact moment of the inception of the process that initiated the stroke could not be determined and no estimates of its propagation speed were obtained.

The same parameters calculated for Case 1 were done for all 15 return strokes, and they are summarized in Table 2. For three among them no peak current estimates were provided by any of the four LF networks. Through the video analysis it is noticeable that their peak luminosities are considerably smaller than most of the other strokes (that could be confirmed by both camera and lightning location systems).

From the third to the fourteenth stroke it was possible to estimate the propagation time spent by the recoil/dart leader to touch ground. By combining that information with the photogrammetric analysis it was possible to obtain average 2-D speeds for those events. The values are listed in Table 2 and they ranged from 1.3 x 10^6 to 9.9 x 10^6 m/s, also in agreement with the available information on both dart and recoil leaders. In Figure 10 the evolution of channel length in function of time is presented. The result is similar to what was shown in figure 6 for Case 1, but the greater amount of points suggests a stronger relationship. By fitting the data linearly, the obtained slope is 18 m/ms, which can be interpreted as the recoil/dart leader inception points are moving away from the vertical channel segment with a speed of 1.8 x 10^4 m/s.

The positive stroke and the subsequent negative strokes of Case 2 occurred approximately 87 and 97 km away from the center of the LMA sensor network, respectively. Similar to Case 1, the resulting data have provided relevant information

on the inception and in-cloud development of each individual stroke and during the time intervals between them. Each individual VHF source that could be detected by SPLMA during the timespan of Case 2 is plotted on Figure 11. The altitude versus time diagram and source rate (number of sources per 10 ms) versus time plot indicate that the number of VHF sources falls dramatically with the negative stroke order. It is reduced to practically none after the sixth touches the ground, suggesting that their channel development below cloud base is completely disconnected from any persisting negative leader branches associated with the inception of the initial positive stroke. This is more evident than the similar behavior reported for Case 1 probably due to the large difference in their multiplicities.

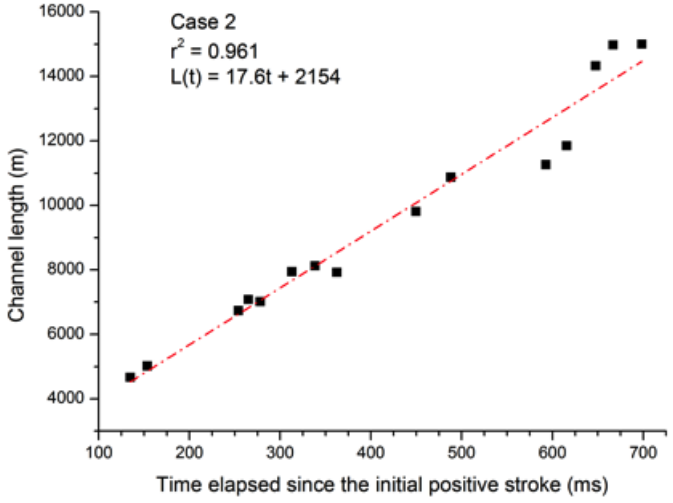

Fig. 10. Total visible channel length (as estimated from the photogrammetric analysis) *versus* time elapsed since the initial positive return stroke for Case 2. Each square corresponds to one of the fifteen negative strokes.

The conclusion of the LMA analysis, for both cases, indicates that the positive strokes played a fundamental role in the formation of the negative strokes on the bipolar CG flashes. However, after their initiation, the negative strokes behave like an independent negative CG flash, but in a smaller scale, and are no longer connected to the development of the in-cloud negative leader of the double-ended tree associated with the bidirectional inception of the initial positive stroke.

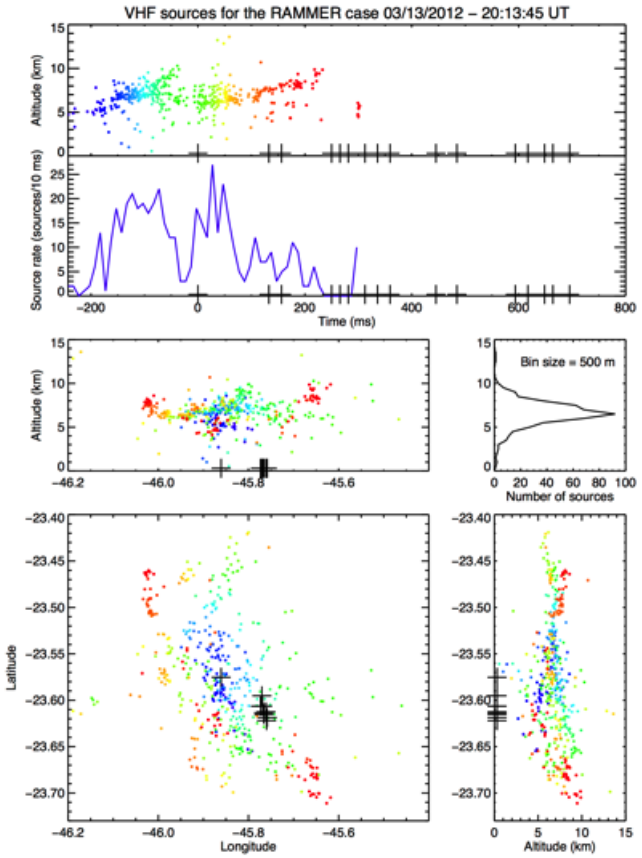

Fig. 11. Same as Figure 7 but for the VHF sources detected for Case 2.

TABLE II. SUMMARY OF CHARACTERISTICS OF EACH OF THE SIXTEEN RETURN STROKES OBSERVED ON CASE 2. I_P CORRESPONDS TO THE PEAK CURRENTS, D IS THE DISTANCE BETWEEN THE STROKES AND THE CAMERA, L_{TOTAL} IS THE TOTAL VISIBLE CHANNEL LENGTH AND RL/DL SPEED IS THE ESTIMATED EXTENSION SPEED OF THE RECOIL/DART LEADER SEQUENCE THAT INITIATED EACH STROKE. N/A STANDS FOR NO DATA AVAILABLE.

Order	**Time of occurrence (UT)**	**Estimated peak current (kA)**				**D (km)**	**L_{total} (m)**	**RL/DL speed (x10^6 m/s)**
		BrasilDAT	***GLD360***	***LINET***	***TLS200***			
Positive	20:13:45.906s (t = 0)	+25.6	+44.1	+34.5	+30.3	47.1	3290	-
1	46.040s (t = 134.8 ms)	–5.47	-	+6.0	–5.2	52.5	4670	-
2	46.059s (t = 153.6 ms)	–3.18	-	–3.3	–3.0	-	5020	-
3	46.160s (t = 254.0 ms)	–6.03	–5.7	–6.1	–5.3	-	6740	1.30
4	46.170s (t = 264.8 ms)	-	-	-	-	-	7080	4.43
5	46.184s (t = 278.0 ms)	–2.93	-	–2.7	-	53.9	7020	4.38
6	46.218s (t = 312.8 ms)	–8.55	–11.0	–9.5	-	53.1	7940	9.93
7	46.244s (t = 338.4 ms)	–3.20	-	–3.5	-	54.2	8120	6.77
8	46.268s (t = 362.4 ms)	–4.27	–5.2	–5.0	-	52.3	7920	4.95
9	46.355s (t = 449.6 ms)	–16.5	–18.8	–18.5	–16.7	53.3	9810	6.13
10	46.394s (t = 448.0 ms)	–4.92	–8.6	–5.0	–4.4	51.0	10870	9.06
11	46.498s (t = 592.8 ms)	–6.44	–6.9	–6.7	–5.5	53.5	11270	9.39
12	46.521s (t = 615.6 ms)	–1.55	-	-	-	-	11850	5.93
13	46.553s (t = 647.6 ms)	–2.29	-	-	-	-	14330	7.16
14	46.572s (t = 666.8 ms)	-	-	-	-	-	14980	6.24
15	46.604s (t = 698.4 ms)	-	-	-	-	-	15000	-

IV. DISCUSSIONS

The uniquely visible features (owing mainly to the elevated cloud base in this time frame) of the two bipolar CG flashes analyzed in the present work make it possible to discuss the physical processes responsible for the creation of the subsequent negative strokes. The two cases are distinct in one important aspect: while Case 1 had the negative strokes following the same channel to ground as the initial positive stroke, Case 2 had all the subsequent negative strokes touching ground through a path that was different from the one created by the initial positive stroke. However, the analysis of the high-speed video records show that, in both cases, recoil leaders initiate the negative return strokes, although in different contexts.

In Case 1 the recoil leaders retraced a channel branch that was originally ionized by the positive leader that set the stage for the initial positive stroke, as illustrated in Figure 12. All the observed recoil events fit into the phenomenology reported by previous researchers [Mazur, 2002; Williams, 2006; Saba et al., 2008; Mazur and Ruhnke, 2011; Warner, 2012; Williams and Heckman, 2012]; one of them, however, propagates toward ground after it reaches the vertical channel segment, instead of moving upward into the cloud base. This process produces a negative return stroke and is subsequently repeated, generating three additional negative strokes. The genesis of the subsequent negative strokes of Case 1 would have been observed as a regular dart leader that followed a path previously created by a positive stroke if the cloud base were lower. It would be similar to the event analyzed in detail by Jerauld et al. [2009], to one of the four events reported by Fleenor et al. [2009] or both events described by Saba et al. [2013]. The high-speed video data of Case 1 is the first direct optical evidence that single-channel bipolar CG flashes are produced as consequence of recoil activity.

The large number of recoil leaders that precede the first subsequent stroke (Figure 5) indicates that they have a cumulative effect in reinforcing the heating and ionization of the remnants of the positive leader branch. During the interstroke intervals between the strokes that followed the first negative CG, no recoil activity was observed in those branches, with the exception of the recoil/dart leader sequences that initiated each of those strokes. This suggests that the heating generated through the entire visible channel by the first negative stroke could make it conductive enough for the following recoil/dart leaders to reach ground without the need of previous recoil events to act as their "precursors".

The analysis of Case 2 suggests that recoil leaders can also be responsible for the creation of a conductive channel for the subsequent negative return strokes that is different from the one followed by the initial positive stroke, possibly after a transition to a stepped propagation mode after leaving the previously ionized channel branches. The high-speed video data shows that part of the channel to ground followed by the first subsequent negative stroke was previously illuminated by at least one recoil leader that occurred during the continuing current period of the initial positive stroke. Instead of reaching the original channel to ground (as observed in Case 1) this recoil/dart leader sequence diverges downwards, eventually touching ground on a different contact point and producing a negative return stroke. If a similar process occurs above cloud base, one would have the situation of three of the four bipolar CG flashes described by Fleenor et al. [2009], in which the subsequent negative strokes created new ground contact points. Unfortunately there is no available fast electric field data for the leader processes, which would make it possible to see if the recoil/dart leader propagates in a stepped fashion after it diverges from the previously ionized channel segment. Also, the high-speed camera frame rate was not high enough to provide multiple estimates of propagation speed, which could reveal the presence of a discontinuity in the speed from the early phase to the final stages of propagation [Campos et al., 2014].

Figure 12 illustrates in detail the mechanism proposed to explain both natural bipolar cloud-to-ground flashes described in the present work. Both flashes initiated between 3 and 5 km altitude, where the respective negative- and positive-dominant charge regions were located. The cartoon also indicates the presence of an extended layer of negative space charge below the cloud base, since they are needed to explain the visible horizontal propagation of the leaders/recoil leaders there. It is conceivable that this negative space charge accumulated in the subcloud region via corona discharge from the Earth's surface in the presence of a strong downward-directed electric field. Each panel of Figure 12 depicts the following processes:

- (A) and (B): The cloud base is located at 3.2 km height, and the flash develops in a bidirectional fashion, with the positive end of the lightning tree propagating towards ground and the negative end developing inside the cloud. The branches in the positive end are usually fainter than in the negative end, and are barely visible with the camera.
- (C): The recoil leaders seem to take place when the faintest branches are about to stop their development, for example, when a current cutoff happened at some point. The recoils act like a current surge on the branch, extending it a little further, and then the branch can propagate for itself again. Such bidirectional nature of the recoil leaders has been previously documented in detail by Warner et al. [2012] and Mazur et al. [2013]. This process can occur on several branches and can repeat on the same one multiple times.
- (D): The lower (positive) end of the bidirectional leader continues to propagate until it touches ground, producing the initial positive return stroke. It is followed by a period of continuing current, which takes place simultaneously with recoil leader activity on positive leader branches that have been cutoff once the return stroke occurred.
- (E): Once the continuing current is finished, the lower section of the double-ended tree is presumed to be cutoff from the in-cloud negative end. The positive charge transfer to ground stops but the negative (upper) end of the in-cloud lightning tree continues to develop independently.

- (F): A large number of recoil leaders (indicated as RL) occur in channel branches visible below cloud base that were previously ionized by the positive leader. Some can reconnect with the active in-cloud negative leader, forming an intracloud discharge, and others are not able to do so.
- (G) and (H): Some of the recoil leaders, in particular, develop towards the vertical section of the channel to ground followed by the positive stroke, behaving as attempted leaders (indicated as RL-AL). Meanwhile, the in-cloud negative leader eventually interrupts its development, as indicated by the VHF sources detected by the SPLMA (Figure 7).
- (I): One of the recoil leaders (that occurred in the region considered for the graph of Figure 5) was capable of following the same path to ground as the initial positive stroke. It behaved as a regular dart leader and produced the first subsequent negative return stroke (indicated as RL-RS). It is important to notice that, from this point on, the horizontal end of the channel carries positive charges and the descending channel carries negative charges to ground.
- (J): Negative charge transfer to ground is finished after the channel cutoff. The positive horizontal end, however, continues to propagate with a luminous emission below the camera sensitivity. As shown previously, the main evidence of this continuous development between strokes is the approximately uniform channel extension documented in Figure 6 (and Figure 10 for Case 2).
- (K): At some point the positive leader propagation is terminated due to current cutoff. This allows the initiation of another recoil leader, which propagates bidirectionally towards ground (similarly to the initial positive and the first negative subsequent strokes) at the same time as it develops further the horizontal positive end of the channel.
- (L): The negative end of the recoil leader reaches ground and produces the second negative stroke, behaving as a regular dart leader. After the first negative return stroke, no intense recoil activity was observed on that branch, and each new recoil leader was responsible for another negative return stroke. The new channel behaves like a regular negative flash, but at a smaller scale. Recoil leaders will continue to produce additional negative strokes as long as charges are still available around the positive leader and while the channel length remains stable.

The conditions for the production of new negative strokes are supported by the charge transfers measured by Waldteufel et al. [1980] through field-mill records. Waldteufel et al. [1980] reported a triggered lightning event in which ten return strokes were initiated in a region of clear air, below cloud base. Also, from stroke to stroke, the illuminated channel branches developed spatially, reaching up progressively into the charge region with an estimated speed of 3×10^4 m/s. They interpreted the observations as a positive leader constantly propagating upward, neutralizing the negative charge distribution located below cloud base by means of both leader development and return stroke occurrence. It is reasonable to assume that a similar phenomenon occurred in the events described here, with the horizontal positive leader developing for as long as there was a negative charge distribution below cloud base not only to feed the propagation but also to produce an adequate electric field and to be transferred to ground by each subsequent negative stroke.

Figures 12G to 12L show the scenario of Case 1, which is valid for bipolar CG flashes where strokes of both polarities follow the same channel to ground. Case 2 presented a very similar development as Case 1, the only difference being the fact that the strike points of the subsequent negative strokes followed a different path to ground. The behavior presented in Figures 12A through 12F is exactly the same, but the processes illustrated from Figure 12G onwards have some crucial differences. Figure 13G – L show the differences between Figure12G – L for Case 2. In Case 2, a very large branch presented recoil activity far from the main channel. When the recoil retraced the branch, it diverged to ground in the form of a stepped leader (Figure 13G and 13H), marked as RL – SL (recol leader/stepped lider process), instead of remaining on the main channel. That created the first negative stroke (Figure 13I). All 14 subsequent strokes followed the same path to ground from that point on, cycling through the processes of Figure 13J to 13L following the new ground termination created by the recoil/dart-stepped leader sequence of the first subsequent negative stroke.

Given the recent high-speed video records with evidence that recoil leaders propagate in a bidirectional fashion [Warner et al., 2012; Mazur et al., 2013], the authors suggest that the recoil/dart leader sequence that produces each negative stroke further extends the horizontal channel segment from where it originates. Eventually, current cutoff occurs, interrupting charge transfer to ground after the negative stroke. However, it seems that the positive leader at the upper end of the channel continues to propagate horizontally, and this action may serve to restress the cutoff segment to new breakdown. This is suggested by the temporal evolution of the visible channel length, which grows at a rate of 10^4 m/s between subsequent strokes (Figures 6, 10, 12J and 13J). Additionally, Waldteufel et al. [1980] observed a remarkably similar behavior (as commented earlier in this section) and Mazur [2002, Section 2.2 and Figure 5] describes the same behavior for the "development of the unidirectional positive leader, which continues even after current cutoff" right after a return stroke in a regular negative cloud-to-ground flash. Eventually, the positive leader development is interrupted by cutoff, giving rise to the inception of other recoil leaders (Figures 12K and 13K). These recoil leaders, as both case studies have shown, retrace the whole channel to ground and set the stage for the subsequent negative strokes (Figures 12L and 13L).

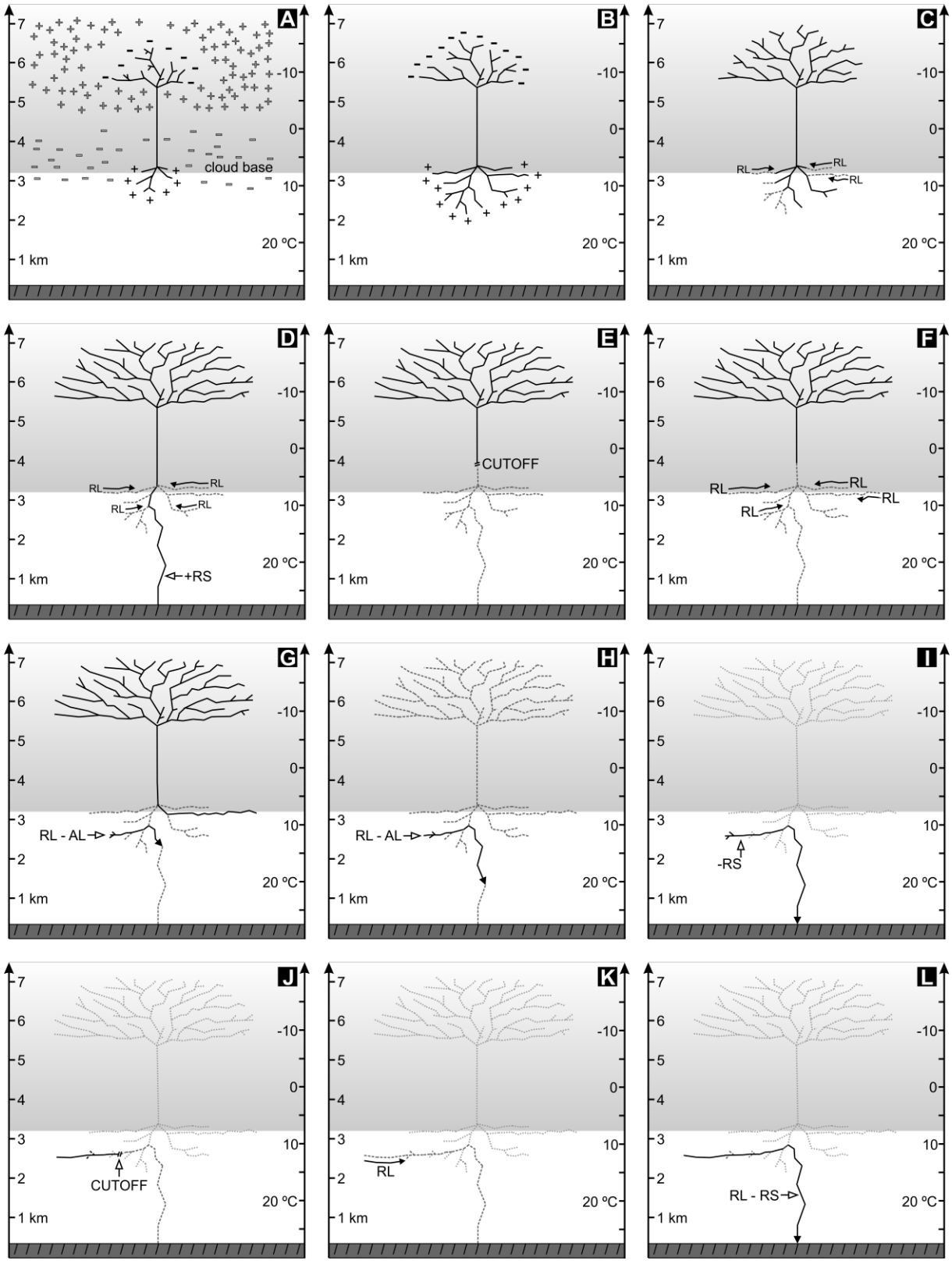

Fig. 12. Illustration of the mechanism proposed to explain natural bipolar cloud-to-ground flashes. Each panel is discussed in detail in the main text body. The two minus signs represent a single charge region, partially inside the cloud and partially outside the cloud. The elaboration of the figure was based mainly on Case 1 and the main differences found on Case 2 are discussed in this section and illustrated on Figure 13.

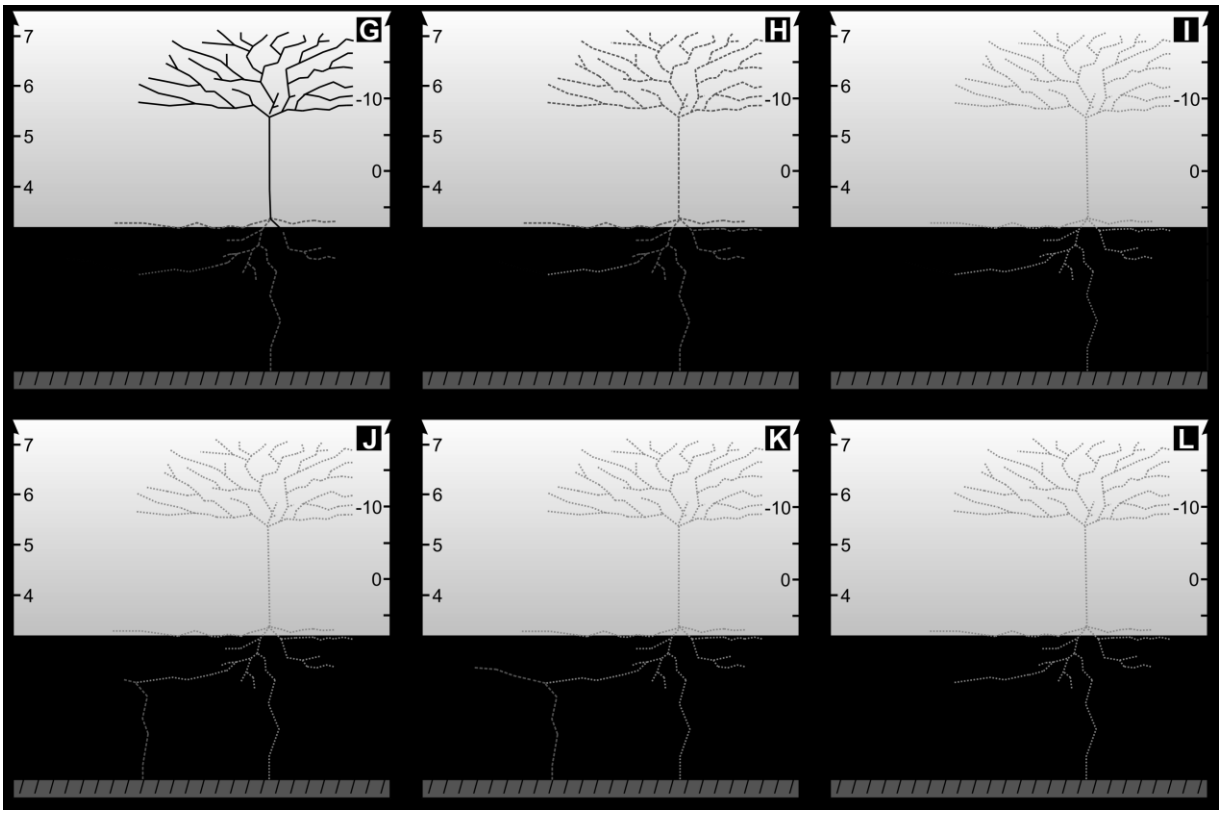

Fig. 13. Same mechanism illustrated in Figure 12A – K, but showing only the divergence occurred when the subsequent strokes create a new path to the ground (G – L).

V. Concluding Remarks

This work analyzed two temporally close bipolar cloud-to-ground flashes observed in São José dos Campos, southeastern Brazil, during the summer of 2012. One high-speed camera of the RAMMER network and several other instruments installed during that summer, as part of the CHUVA campaign, observed these events. Due to the elevated cloud base height, the cameras were able to record the entire development of the subsequent negative strokes below cloud base in both cases. Also, each case presented different behaviors: while in Case 1 all subsequent strokes shared the same final channel section to ground, Case 2 had different ground contact points for the main positive CG stroke and the subsequent negative CG strokes. The joint analysis of the high-speed camera, LMA and LLS data allowed the elaboration of a conceptual empirical inception mechanism of subsequent negative strokes in natural downward bipolar flashes (Figures 12 and 13). The main results were:

- The first optical evidence that both single- and multiple-channel bipolar flashes occur as a consequence of recoil leader activity in the branches of the initial positive return stroke.
- The total channel length of the negative strokes increased progressively with time. The channel growth rate was equivalent to a propagation speed of the order of 10^4 m/s. Such speed corresponds to positive leaders observed under many different circumstances. The most probable mechanism is that the positive end of the leader continuously propagates until the point where it becomes faint and eventually stops, possibly due to current cutoff.
- At the verge of a channel current cutoff or right after it has taken place, recoil leaders might act on the channels like current surges, feeding the channel and also extending it a little further. From that point on, the channel can continue its self-propagation, produce more recoil leaders or completely fade away and stop its extension.
- By analyzing the LMA data it was possible to show that all the subsequent strokes had no connection with the upper in-cloud negative leader created during the bidirectional development of the initial return stroke.

Cases 1 and 2 also presented a few distinctive features:

- Case 1: A large number of recoil leaders (close to twenty) occurred in the same channel segment after the initial positive stroke until one of them could strike ground. This indicates that the cumulative effect of ionization and heating by the developing recoil leaders was important in creating the adequate conditions for one of them to finally produce a negative stroke.
- Case 2: In this case, however, the recoil/dart leader in development leaves the original path, creating a new branch and eventually contacting ground.

Even though this mechanism was proposed based on two events whose negative strokes had their preparatory process observed by a high-speed camera below cloud base, it can also be extended to the more general case of bipolar CG flashes. All the natural cloud-to-ground events that have been reported previously [Fleenor et al., 2009; Jerauld et al., 2009; Saba et al., 2012] can be described by this mechanism if one considers that the recoil leaders responsible for the subsequent negative strokes also occur above cloud base.

ACKNOWLEDGMENT

The authors would like to thank UNIVAP (Universidade do Vale do Paraíba) and Rede Vanguarda de Televisão for their support in hosting the sensors during the observations and helping with maintenance. The authors are also grateful to all CHUVA participants responsible for the installation and maintenance of the several sensors present at the 2012 campaign and whose data were vital to the development of this work.

REFERENCES

Berger, K., and E. Vogelsanger (1965), Messungen und Resultate der Blitzforschung der Jahre 1955-1963 auf dem Monte San Salvatore, Bull. Schweiz. Eletrotech. Ver., 56, 2-22.

Berger, K., and E. Vogelsanger (1966), Photographische Blitzuntersuchungen der Jahre 1955-1963 auf dem Monte San Salvatore, Bull. Schweiz. Elektrotech. Ver., 57, 599-620.

Betz, H.-D., K. Schmidt, W. P. Oettinger, and M. Wirz(2004), Total VLF/LF-lightning and pseudo 3D-discrimination of intra-cloud and cloud-to-ground discharges, paper presented at 18th International Lightning Detection Conference, Vaisala, Helsinki,Finland.

Campos, L. Z. S., M. M. F. Saba, T. A. Warner, O. Pinto Jr., E. P. Krider and R. E. Orville (2014), High-speed video observations of natural cloud-to-ground lightning leaders – A statistical analysis, Atmos. Res., 135-136, 285-305, doi:10.1016/j.atmosres.2012.12.011.

Demetriades, N. W. S., M. J. Murphy, and J. A. Cramer (2010), Validation of Vaisala's Global Lightning Dataset (GLD360) over the continental United States, paper presented at 21st International Lightning Detection Conference, Vaisala, Orlando, Florida.

Fleenor, S. A., C. J. Biagi, K. L. Cummins, E. P. Krider, and X. M. Shao (2009), Characteristics of cloud-to-ground lightning in warm-season thunderstorms in the Central Great Plains, Atmos. Res., 91, 333-352, doi:10.1016/j.atmosres.2008.08.011.

Hubert, P., A. Eybert-Berard, and L. Barret (1984), Triggered lightning in New Mexico, J. Geophys. Res., 89, 2511-2521.

Idone, V. P., R. E. Orville, D. M. Mach and W. D. Rust (1987), The propagation speed of a positive lightning return stroke, Geophys. Res. Lett., 14, p.1150-1153.

Jerauld, J. E., M. A Uman, V. A. Rakov, K. J. Rambo, D. M. Jordan, and G. H. Schnetzer (2009), Measured electric and magnetic fields from an unusual cloud-to-ground lightning flash containing two positive strokes followed by four negative strokes, J. Geophys. Res., 114, D19115, doi:10.1029/2008JD011660.

Jordan, D. M., V. P. Idone, V. A. Rakov, M. A. Uman, W. H. Beasley, and H. Jurenka (1992), Observed dart leader speed in natural and triggered lightning, J. Geophys. Res., 97, 9951-9957.

Kasemir, H. W. (1950), Qualitative Ubersicht uber Potential-, Feld- und Ladungsverhaltnisse bei einer Blitzentladung in der Gewitterwolke, in Das Gewitter, edited by H. Israel, pp. 112 –126, Akad. Verlagsges., Leipzig, Germany.

Kasemir, H. W. (1960), A contribution to the electrostatic theory of a lightning discharge, J. Geophys. Res., 65, 1873-1878.

Krehbiel, P. R. (1981), An analysis of the electric field change produced by lightning, Ph.D. thesis, Dep. of Pure and Appl. Phys., Univ. Manchester, Manchester, England.

Krehbiel, P. R., M. Brook, and R. A. McCrory (1979), An analysis of the charge structure of lightning discharges to ground, J. Geophys. Res., 84, 2432-2456

Krider, E. P. (1974), An unusual photograph of an air lightning discharge, Weather, 29, p.24-27.

Machado, L. A. T., A. Calheiros, E. Mattos, I. Costa, D. Vila, R. Albrecht, C. Morales, C. Angelis, M. Silva Dias and G. Fisch (2012), Tropical cloud processes : First results from CHUVA Project, paper presented at 16th International Conference on Clouds and Precipitation (ICCP2012), Leipzing, Germany.

Mazur, V. (2002), Physical processes during the development of lightning flashes, C. R. Physique, 3, 1393-1409.

Mazur, V., and L. H. Ruhnke (2011), Physical processes during development of upward leaders from tall structures, J. Electrostat., 69, 97-110, doi:10.1016/j.elstat.2011.01.003.

Mazur, V., L. H. Ruhnke, T. A. Warner, and R. E. Orville (2013), Recoil leader formation and development, J. Electrostat., in press, doi:10.1016/j.elstat.2013.05.001.

McEachron, K. B. (1939), Lightning to the Empire State Building, J. Franklin Inst., 227, 149-217.

Naccarato, K.P.; A. C. V. Saraiva, M. M. F. Saba, C. Schumann and O. Pinto Jr. (2012), First Performance Analysis of Brasildat Total Lightning Network in Southeastern Brazil, paper presented at International Conference On Grounding And Earthing (GROUND'2012), Bonito, Brazil.

Nag, A., and V. A. Rakov (2012), Positive lightning: An overview, new observations, and inferences, J. Geophys. Res., 117, D08109, doi:10.1029/2012JD017545.

Nakahori, K., T. Egawa, and H. Mitani (1982), Characteristics of winter lightning currents in Hokuriku district, IEEE Trans. Power Appar. Syst., 101, 4407-4412.

Orville, R. E., and V. P. Idone (1982), Lightning leader characteristics in the Thunderstorm Research International Program (TRIP), J. Geophys. Res., 87, 11,177-11,192.

Rakov, V. A. (2003), A review of positive and bipolar lightning discharges, Bull. Amer. Meteor. Soc., 84, 767-776, doi:10.1175/BAMS-84-6-767.

Rison, W., R. J. Thomas, P. R. Krehbiel, T. Hamlin and J. Harlin (1999), A GPS-based three-dimensional lightning mapping system: Initial observations in central New Mexico, Geophys. Res. Lett., 26, 3573-3576.

Saba, M. M. F., K. L. Cummins, T. A. Warner, E. P. Krider, L. Z. S. Campos, M. G. Ballarotti, O. Pinto Jr., and S. A. Fleenor (2008), Positive leader characteristics from high-speed video observations, Geophys. Res. Lett., 35, L07802, doi:10.1029/2007GL033000.

Saba, M. M. F., C. Schumann, T. A. Warner, J. H. Helsdon Jr., W. Schulz, and R. E. Orville (2013), Bipolar cloud-to-ground lightning flash observations, J. Geophys. Res. Atmos., 118, 11,098–11,106, doi:10.1002/jgrd.50804.

Saraiva, A. C. V., O. Pinto Jr, M. Ferreira, G. S. Zepka, and M. M. F. Saba (2011), RAMMER Project: First observations of the high speed camera network to monitor and study lightning, paper presented at the XIV International Conference on Atmospheric Electricity, Rio de Janeiro, Brazil.

Schonland, B. F. J., D. J. Malan, and H. Collens (1935), Progressive lightning, 2, Proc. Roy. Soc. (Lond.), A152, 595-625.

Shao, X. M., P. R. Krehbiel, R. J. Thomas, and W. Rison (1995), Radio interferometric observations of cloud-to-ground lightning phenomena in Florida, J. Geophys. Res., 100, 2749-2783.

Waldteufel, P., P. Metzger, J.-L. Boulay, P. Laroche, and P. Hubert (1980), Triggered lightning strokes originating in clear air, J. Geophys. Res., 83, 2861-2868.

Warner, T. A. (2012), Observations of simultaneous upward lightning leaders from multiple tall structures, Atmos. Res., 117, 45-54, doi:10.1016/j.atmosres.2011.07.004.

Warner, T. A., M. M. F. Saba, and R. E. Orville (2012), Characteristics of upward leaders from tall towers, paper presented at 22nd International Lightning Detection Conference, Vaisala, Broomfield, CO.

Williams, E., and Y. Yair (2006), The microphysical and electrical properties of sprite-producing thunderstorms, in Sprites, Elves and Intense Lightning Discharges, edited by M. Füllekrug et al., pp. 57-83, Springer, Dordrecht, Netherlands, doi:10.1007/1-4020-4629-4_3.

Williams, E., and S. Heckman (2012), Polarity asymmetry in lightning leaders: the evolution of ideas on lightning behavior from strikes to aircraft, AerospaceLab Journal, 5, p. AL05-04.

Zipser, E. J. (1977), Mesoscale and convective-scale downdrafts as distinct components of squall-line structure, Mon. Wea. Rev., 105, 1568–1589, doi:10.1175/1520-0493(1977)105<1568:MACDAD>2.0.CO;2.